J|A|C|S COMMUNICATIONS

Published on Web 11/22/2010

Oxygen Plasma Etching-Induced Crystalline Lattice Transformation of Colloidal Photonic Crystals

Tao Ding,[†,§] Fei Wang,[‡,§] Kai Song,[*,†] Guoqiang Yang,[†] and Chen-Ho Tung[†]

Key Laboratory of Photochemistry and Joint Laboratory of Polymer Science and Materials, Beijing National Laboratory for Molecular Sciences, Institute of Chemistry, Chinese Academy of Sciences, Beijing 100190, China, and Graduate University of the Chinese Academy of Sciences, Beijing 100049, China

Received July 27, 2010; E-mail: kai.song@iccas.ac.cn

Abstract: This communication describes the transformation of a colloidal crystalline lattice that was realized via oxygen plasma etching of colloidal crystals made of SiO_2@PMMA core−shell microspheres. The plasma etching of the colloidal crystals proceeded nonuniformly from the top to the bottom of the colloidal crystals. The PMMA shell was etched away by the oxygen plasma in a layer-by-layer manner, and the silica core was drawn into the pit formed by the neighboring spheres in the layer below. Consequently, the crystalline lattice was transformed while the order was maintained. Scanning electron microscopy images and reflection spectra further confirmed the change in the crystalline structures. Colloidal crystals with sc and bcc lattices can be fabricated if the ratio of the polymer shell thickness to the silica core diameter is equal to certain values. More importantly, this approach may be applicable to the fabrication of various assembly structures with different inorganic particles.

Colloidal crystals (CCs) have received great attention in recent years because of their significant applications in photonics,[1] catalysis,[2] templates,[3] and sensors.[4] Typically, they have served as colloidal photonic crystals for manipulating the transmission of light via the photonic band gap (PBG). In most of these cases, the artificial three-dimensional (3D) CCs obtained predominantly have the face-centered-cubic (fcc) crystalline structure, which is energetically favorable. It has been suggested that only a pseudo-PBG exists in an fcc lattice, no matter how high the refractive-index contrast is; this is caused by the symmetry-induced degeneracy of the photonic bands.[5] Therefore, CCs with new symmetries are highly desired to realize the complete PBG in the visible region. To this end, early research in this direction mainly focused on two strategies. One is "post-crystallization treatment", which deforms colloidal building blocks from spheres to ellipsoids or oblates after their self-assembly into colloidal crystals.[6] The other is the direct self-assembly of nonspherical colloidal particles.[7]

Besides all of the above, fabrication of CCs with crystalline lattices other than fcc (e.g., diamond, triclinic, etc.), which would be beneficial for broadening the PBGs, can be regarded as an alternative approach to break the symmetry of the fcc lattice and reach complete PBGs. In comparison with the fcc lattice, these crystalline lattices have lower filling fractions (which is also helpful for broadening the PBGs) but are not energetically favorable for fabrication by the self-assembly method.[8] Because of this, only a few groups have made progress toward this goal, including fabricating CCs with triclinic, simple cubic (sc), body-centered cubic (bcc), and diamond lattices.[9] However, more general and practical strategies are still desirable.

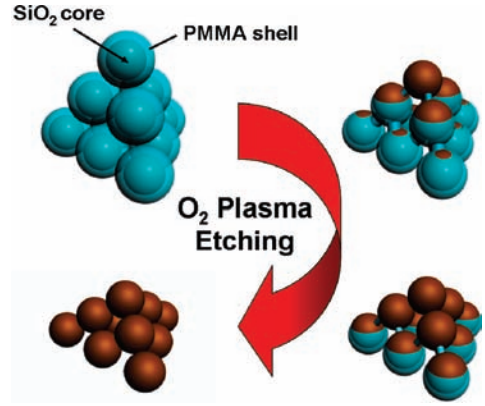

Figure 1. Schematic illustration of the transformation of the crystalline lattice from fcc to sc induced by oxygen plasma etching.

Herein, we adopted SiO_2@PMMA core−shell spheres as the building blocks to form 3D CCs with the fcc lattice. When the CCs were subjected to nonuniform oxygen plasma etching in which the etching rate decreased in going from the top to the bottom of the CCs,[10] the poly(methyl methacrylate) (PMMA) shells were removed in a layer-by-layer manner, and the silica cores were trapped in the pits formed by the neighboring spheres in the layer below in such a stepwise procedure. As a result, non-close-packed CCs with changed crystalline lattices were formed, as schematically illustrated in Figure 1. The resulting crystalline lattice can be tuned simply by controlling the ratio of the polymer shell thickness to the silica core diameter and the orientation of the CCs.

First, monodisperse SiO_2@PMMA core−shell microspheres with a core diameter of ∼250 nm and a shell thickness of ∼20 nm were synthesized as described in the literature,[11] and their structure was confirmed by transmission electron microscopy (TEM) (Figure 2a inset). Next, CCs made of core−shell spheres were fabricated via the convective self-assembly method.[12] The assembled opal structure presented good 3D order with the (111) crystalline plane parallel to the substrate, as shown in Figure 2a. After 40 min of oxygen plasma etching, the non-close-packed CCs with changed crystalline lattices were formed (Figure 2c, e).

During the etching process, the etching rate decreased in going from the top to the bottom of the CCs.[10a] Also, in each layer, the polymer shell exposed to the surface was etched first, while the etching rate was lower in the contact region between two neighboring spheres. As a result, polymer necks were formed between the silica spheres.[10b] These tubular necks were subjected to melting

[†] Key Laboratory of Photochemistry, Beijing National Laboratory for Molecular Sciences.
[‡] Joint Laboratory of Polymer Science and Materials, Beijing National Laboratory for Molecular Sciences.
[§] Graduate University of the Chinese Academy of Sciences.

10.1021/ja106657t

and deformation caused by the high temperature when the oxygen plasma was processed,[13] which resulted in the relocation and shrinking of each silica sphere into the trigonal pit formed by the three spheres in the layer below. Consequently, the distance between the neighboring layers was decreased. On the other hand, the shrinkage of the silica cores in the same layer was not as severe as that between the neighboring layers because of the templating effect from the layer below, which trapped the silica from moving horizontally. Finally, as a result of the low etching rate and layer-by-layer shrinkage, the long-range order was well-preserved, although some defects existed, as shown in Figure 2c. These defects were mainly caused by a sidewise shift of silica spheres away from the center of the pits, which resulted from nonuniform shrinking. One suggested solution to this problem would be to use low-temperature plasma etching to avoid the sidewise shift of spheres.[13] However, this is not reachable in our laboratory under current conditions.

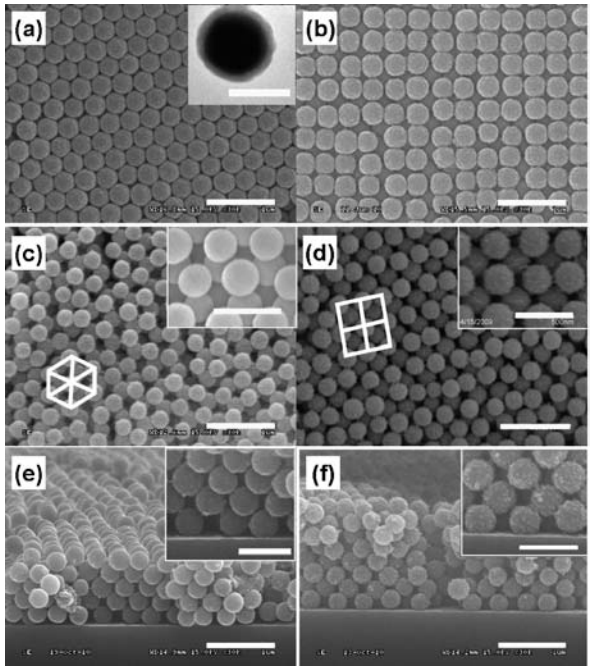

Figure 2. SEM images of SiO_2@PMMA opal. (a) Image with (111) upward. The inset shows a TEM image of a core−shell sphere. (b) Image with (100) upward. (c, d) Top views of the etched non-close-packed CCs corresponding to (a) and (b), respectively. The white lines are guides to the eyes. (e, f) Side views of the etched non-close-packed CCs corresponding to (a) and (b), respectively. The insets in (c−f) are magnified views of the non-close-packed lattices. Scale bars: main images, 1 μm; inset in (a), 250 nm; insets in (c−f), 500 nm.

The Bragg peak measured from the (111) crystalline plane was also blue-shifted after plasma etching, as shown in Figure 3. The original silica opal presented a strong Bragg peak at 563 nm. When core−shell microspheres with a shell thickness of ~20 nm were used as building blocks, the Bragg peak of the composite CC was red-shifted to 660 nm. After the plasma etching, the reflection peak was blue-shifted from 660 to 510 nm, which should be due to the joint effect of lowering the volume fraction of the dielectrics and decreasing the distance between the two neighboring crystalline planes. In comparison with the reflection peak for the bare silica opal having the same silica spheres as building blocks (dashed line in Figure 3), the reflection peak of the silica CCs with the triclinic lattice was blue-shifted by ~50 nm, which we believe is caused by the decreased distance between the two neighboring (111) planes and the lower filling fraction of the dielectrics in this triclinic structure than in fcc structure. The Bragg peak position of a CC can be approximately calculated using the Bragg equation for diffraction under normal incidence. The calculated Bragg peak position of the etched CC was at 491 nm, which is basically in agreement with the measured value. Meanwhile, the reflection strength was weakened, which was mainly caused by the defects introduced during plasma etching. It is noteworthy that the lower filling fraction in the etched structure theoretically should result in sharp, intense stop bands. Reasonably, the thinner the shell is etched, the better the order can be preserved. Here we compared the optical properties of etched non-close-packed colloidal crystals and found that the reflection intensity of the etched structure from the core−shell CC with thickness of 10 nm is stronger than the original one. Furthermore, increasing shell thickness resulted in a weaker reflection intensity (see Figures S2 and S3 in the Supporting Information).

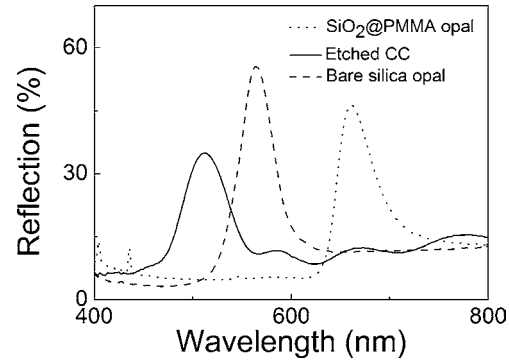

Figure 3. Reflection spectra of composite SiO_2@PMMA CCs before (dotted line) and after (solid line) plasma etching for 40 min. The dashed line represents the reflection spectrum of the bare silica opal assembled from silica sphere building blocks identical to the silica cores in the composite CCs.

The spectra can be further tuned by adjusting the thickness of the polymer shell. It is noteworthy that when the polymer shell thickness (h) had the value $h = 0.207D_0$, where D_0 is the silica core diameter, CCs with the sc crystalline lattice can be obtained (see the Supporting Information for details). It was reported that the sc crystalline lattice had the potential to realize the complete PBG in the visible region,[14] and further investigation is underway.

We also applied this technique to obtain other colloidal crystalline lattice. First, the CCs with the (100) crystalline plane parallel to the substrate were fabricated following the literature.[15] After the PMMA shell was etched away, the silica cores fell into the square pits formed by the four neighboring spheres in the layers below. The transformation of the (100) crystalline planes is clearly demonstrated in Figure 2b and Figure 2d,f, which show the lattice before and after plasma etching, respectively. However, the Bragg peak cannot be detected from (100) planes because no pseudogap opens at the X point of the reciprocal lattice of an fcc structure.[8b,16] It is noteworthy that when the polymer shell thickness (20 nm) approximately corresponded to the value $h = 0.077D_0$ (with $D_0 =$ 250 nm), a bcc crystalline lattice was obtained (see the Supporting Information for details).

In conclusion, we have introduced a novel and practical way to fabricate CCs with triclinic, sc, and bcc lattices by applying oxygen plasma etching to the opal structure of SiO_2@PMMA composite microspheres. The crystalline lattice can be tuned by simply controlling the ratio of polymer shell thickness to the silica core diameter of the synthesized core−shell particles. Both the reflection

spectra and SEM images verified the transformation of the crystalline structures. These non-close-packed CCs also show a prominent broader band gap relative to fcc colloidal photonic crystals.[17] Furthermore, this approach also holds promise for the realization of various non-close-packed assembly structures of other inorganic particles.

Acknowledgment. This work was supported by the NSFC (60877032) and the 973 Project (2007CB808004, 2009CB930802). We also thank the Key Laboratory of Photochemical Conversion and Optoelectronic Materials, TIPC, CAS.

Supporting Information Available: Experimental details, TEM image of the SiO_2@PMMA colloids, detailed calculation of Bragg peaks, the relationship between h and D_0 for the sc and bcc crystalline lattices, SEM images of etched SiO_2@PMMA CCs with shell thickness of 10 nm, and reflection spectra of a series of etched CCs with different original shell thickness. This material is available free of charge via the Internet at http://pubs.acs.org.

References

(1) Marlow, F.; Muldarisnur; Sharifi, P.; Brinkmann, R.; Mendive, C. *Angew. Chem., Int. Ed.* **2009**, *48*, 6212.
(2) Yu, J.-S.; Kang, S.; Yoon, S. B.; Chai, G. *J. Am. Chem. Soc.* **2002**, *124*, 9382.
(3) Xia, Y.; Gates, B.; Yin, Y.; Lu, Y. *Adv. Mater.* **2000**, *12*, 693.
(4) Holtz, J. H.; Asher, S. A. *Nature* **1997**, *389*, 829.
(5) Biswas, R.; Sigalas, M. M.; Subramania, G.; Ho, K.-M. *Phys. Rev. B* **1998**, *57*, 3701.
(6) (a) Jiang, P.; Bertone, J. F.; Colvin, V. L. *Science* **2001**, *291*, 453. (b) Velikov, K. P.; van Dillen, T.; Polman, A.; van Blaaderen, A. *Appl. Phys. Lett.* **2002**, *81*, 838. (c) Lu, Y.; Yin, Y.; Li, Z.-Y.; Xia, Y. *Langmuir* **2002**, *18*, 7722. (d) Ding, T.; Liu, Z.; Song, K.; Clays, K.; Tung, C.-H. *Langmuir* **2009**, *25*, 10218.
(7) (a) Hosein, I. D.; Liddell, C. M. *Langmuir* **2007**, *23*, 8810. (b) Hosein, I. D.; Liddell, C. M. *Langmuir* **2007**, *23*, 10479. (c) Ding, T.; Song, K.; Clays, K.; Tung, C.-H. *Adv. Mater.* **2009**, *21*, 1936. (d) Ding, T.; Song, K.; Clays, K.; Tung, C.-H. *Langmuir* **2010**, *26*, 11544. (e) Riley, E. K.; Liddell, C. M. *Langmuir* **2010**, *26*, 11648.
(8) (a) Xia, Y.; Gates, B.; Li, Z.-Y. *Adv. Mater.* **2001**, *13*, 409. (b) López, C. *Adv. Mater.* **2003**, *15*, 1679. (c) Gailot, D. P.; Summers, C. J. *J. Appl. Phys.* **2006**, *100*, 113118. (d) Hynninen, A.-P.; Thijssen, J. H. J.; Vermolen, E. C. M.; Dijkstra, M.; van Blaaderen, A. *Nat. Mater.* **2007**, *6*, 202.
(9) (a) García-Santamaría, F.; Miyazaki, H. T.; Urquía, A.; Ibisate, M.; Belmonte, M.; Shinya, N.; Meseguer, F.; López, C. *Adv. Mater.* **2002**, *14*, 1144. (b) Li, F.; Delo, S. A.; Stein, A. *Angew. Chem., Int. Ed.* **2007**, *46*, 6666. (c) Dziomkina, V.; Hempenius, M. A.; Vancso, G. J. *Polymer* **2009**, *50*, 5713.
(10) (a) Freyman, G. V.; John, S.; Kitaev, V.; Ozin, G. A. *Adv. Mater.* **2005**, *17*, 1273. (b) Ding, T.; Song, K.; Clays, K.; Tung, C.-H. *Langmuir* **2010**, *26*, 4535.
(11) Ruhl, T.; Spahn, P.; Hermann, C.; Jamois, C.; Hess, O. *Adv. Funct. Mater.* **2006**, *16*, 885.
(12) Jiang, P.; Bertone, J. F.; Hwang, K. S.; Colvin, V. L. *Chem. Mater.* **1999**, *11*, 2132.
(13) Plettl, A.; Enderle, F.; Saitner, M.; Manzke, A.; Pfahler, C.; Wiedemann, S.; Ziemann, P. *Adv. Funct. Mater.* **2009**, *19*, 3279.
(14) Sozuer, H. S.; Haus, J. W. *J. Opt. Soc. Am. B* **1993**, *10*, 296.
(15) Zhang, T.; Tuo, X.; Yuan, J. *Langmuir* **2009**, *25*, 820.
(16) Mihi, A.; Ocaña, M.; Míguez, H. *Adv. Mater.* **2006**, *18*, 2244.
(17) Meseguer, F.; Fenollosa, R. *J. Mater. Chem.* **2005**, *15*, 4577.

JA106657T